NEW 3D-CALCULATIONS OF RESIDUAL STRESSES CONSISTENT WITH MEASURED RESULTS OF THE IIW ROUND ROBIN PROGRAMME

T. LOOSE*, J. SAKKIETTIBUTRA** and H. WOHLFAHRT***

**Ingenieurbüro Tobias Loose GbR*
***Bremer Institut für angewandte Strahltechnik GmbH*
**** Institut für Füge- und Schweißtechnik, TU Braunschweig*

ABSTRACT

The joint working group "Residual Stresses" of IIW commissions X, XIII and XV has carried out a Round Robin Programme on calculation and measurement of residual stresses in an austenitic steel plate (steel type 316L, 270 x 200 x 30 mm^3, TIG welded, two deposits). Measurements by means of X-ray diffraction, neutron diffraction, with the hole drilling method and with electron Speckle-interferometry have revealed pronounced maxima of the longitudinal residual stresses up to more than 500 MPa in the heat affected zone (HAZ). But it is completely unsatisfying that calculations of all contributors using kinematic hardening as material law have not been able to detect such maxima in the HAZ. Only a rather broad horizontal plateau of tensile residual stresses with magnitudes in the range of the yield strength at room temperature (σ_{yield} = 275 MPa, $\sigma_{residual\ stress}$ = 240 MPa to 290 MPa) was shown from the calculations.

Now new 3D-calculations using isotropic hardening in connection with the SYSWELD programme indicate distributions of the longitudinal – and also the transverse – residual stresses which are convincingly consistent with the results of the measurements. The agreement is especially good if one compares the calculations with measurements integrating the residual stresses over the same depth as the depth dimension of the calculation elements is.

The paper about these new comprehensive calculation results presents the total distribution of longitudinal and of transverse residual stresses not only in graphs of the top side after cooling, but also at different time steps during the process. With additional calculations of the von Mieses stresses, strain hardening, deformations, elastic and plastic strains the origin of the residual stress maxima and minima in the HAZ and in the weld seam of the plate can be explained. It has to be discussed whether it is good enough to use pure isotropic hardening in the constitutive law to get correct results or whether a mixed hardening concept should be used.

Additional calculations in the paper demonstrate that the pronounced maxima of longitudinal residual stresses can actually not be found with a kinematic hardening concept. Thus the paper offers arguments that calculations with kinematic hardening may overestimate the influence of the Bauschinger effect especially for materials with a rather high strain hardening exponent like austenitic steels. Such an overestimation could consequently result in an underestimation of the yield strength after the first reversal of the load, that is to say, in the cooling period of the HAZ. Therefore an increase of the yield strength due to strain hardening in the HAZ could be limited incorrectly and the local development of higher tensile residual

stresses in the HAZ would also be limited incorrectly. The result could be a flat horizontal plateau of residual stresses, as in the older calculations, instead of a stress maximum.
The results show that the strict use of the kinematic hardening law is not advisable in any case for the calculation of welding stresses. As a more general result the new calculations and the discussed arguments should allow to present some advices about the use of the kinematic hardening law, the isotropic hardening law or more complicated mixed hardening material laws depending upon the material to be considered. All together this will finally be a quite encouraging result of the IIW Round Robin Programme.

INTRODUCTION

The International Institute of Welding (IIW) has carried out Round Robin investigations on the residual stresses in an austenitic steel plate. The aim was to check the applicability of calculation methods as well as of measuring techniques and finally to compare the results of calculations and of measurements [1].

As it is well known that a strong Bauschinger effect has to be attributed to an austenitic material, it seemed quite reasonable to use the kinematic hardening model, which takes into account this effect, for the calculations. But after completion of residual stress measurements with X-ray and neutron diffraction and with various hole drilling techniques striking discrepancies became obvious between the calculated and the measured longitudinal residual stresses. All measurements revealed a relative minimum of the longitudinal residual stresses at the centre line of the weld seam and maxima in distances between 5 and 8 mm from the centre line. These maxima are with magnitudes up to 500 MPa most pronounced in a thin surface layer (X-ray measurements), but maxima with smaller magnitudes have been found also in deeper layers, for instance in a depth below surface of 3 mm with ca. 300 MPa (neutron diffraction measurements) [2]. The calculated longitudinal residual stresses reveal neither a minimum at the weld centre line nor a maximum in a distance between 5 mm and 8 mm from the weld centre line. Only a rather broad horizontal plateau of tensile residual stresses or a small maximum at the weld centre line with magnitudes in the range of the yield strength at room temperature (σ_{yield} = 275 MPa, $\sigma_{residual\ stress}$ = 240 – 290 MPa) could be found by the calculations using the kinematic hardening model [3, 4]. Concerning the transverse residual stresses the discrepancies between calculated and measured distributions can be considered as not so fundamental. Measurements as well as calculations indicate minima at the weld centre line, partly in the compressive range, and flat tensile maxima in certain distances from the weld centre line – although the calculated distances are in the wide range between 10 mm and nearly 30 mm and the magnitudes between 60 MPa and 180 MPa in comparison with measured distances between 10 mm and ca. 20 mm and magnitudes between 100 MPa and the exceptional value of 300 MPa measured by means of X-rays [2, 3, 4]. Fig. 1 presents calculated residual stresses in comparison with distributions measured by means of X-rays containing the extremely high maximums values.

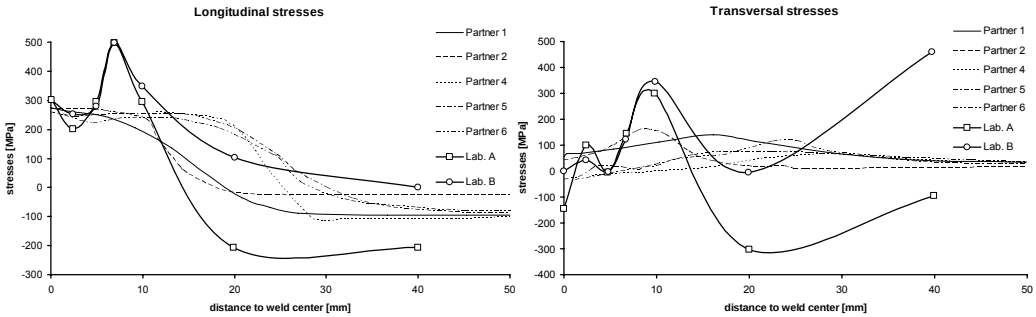

Fig.1 Calculated longitudinal (left) and transverse (right) residual stresses versus distance from the weld centre line in comparison with residual stress distributions measured by means of X-rays [3, 4]

A review of literature suggested however that the efficiency of the Bauschinger effect is not only strongly dependent on the type of the material but also on the temperature at which the deformation process is accomplished. It is for instance recommended to take into account in calculations the hardening behaviour of austenitic steel at room temperature with a combination of isotropic and kinematic hardening in equal percentages [5]. Even more important is the instruction that the influence of the Bauschinger effect decreases for plastic deformations under elevated temperatures (e.g. 480 °C), as they are effective in the HAZ during welding [6].

According to these statements in literature it seemed reasonable to check whether 3D calculations with material laws like isotropic hardening or combinations of kinematic and isotropic hardening would offer a chance to solve the cited problem with the austenitic steel, especially whether the experimentally proven maxima of the longitudinal residual stresses could then also be revealed by calculations [7]. As the results under the assumption of pure isotropic hardening showed the best agreement with measured results, it became obvious, that the choice of the hardening model is most important for the quality of calculations of residual stresses. Further modifications of the calculation models, as for instance the kind of modelling of the filler material (“chewing gum” method or activation of elements) or different variations of modelling the isostatically determined support have less influence on the results. But simplifications with a 2D modelling allow only insufficient results.

The presented result of the new 3D calculations are completed by calculations of the welding induced deformations and work hardening effects, which offer detailed instructions for the understanding of the stress distributions. The good agreement between the results calculated with the use of the isotropic hardening model and measured residual stress distributions can be explained in terms of a pronounced work hardening in the HAZ, the influence of which is excluded by considering the Bauschinger effect in the kinematic hardening model. The results of measurements and calculations of the angular distortion and of a bending round an axis transverse to the seam of the steel plate are cited shortly.

ROUND ROBIN INVESTIGATIONS

For the IIW Round Robin Investigations three plates of the austenitic steel 316L with the dimensions 270 x 200 x 30 mm^3 have been used. Each plate was supported at three points and in a V-shaped groove along the 270 mm long middle line two weld passes have been deposited with tungsten inert gas welding. Details about the welding conditions and the dimensions of the two deposits can be found in [1]. The thermal cycles during welding of both deposits have been controlled by four thermocouples at different positions along the seam and in different distances from the fusion line. The measured thermal cycles during welding in a laboratory of the Electricité de France Company are registered in [1], where also a database of the thermal and mechanical material properties is given. For modelling of the heat input the SYSWELD programme was recommended and for modelling the materials behaviour the kinematic hardening model was pretended. It was proposed to calculate the longitudinal, transverse and radial residual stresses versus the thickness of the plate and along lines transverse to the seam at the top side and the bottom side of the plate.

CALCULATION METHODS

The described 3D thermo-mechanical simulations are performed with the commercial finite element programme SYSWELD 2008.1. The plate is discretised by 55.000 linear volume elements of the type “3008”. The elements representing the weld pool have an edge-length of 1 mm. Figure 2 shows the surface and a cross-section of the finite element mesh. The elements representing the filler material are modelled and activated from the beginning of the process. Before welding, the filler-material has the material properties of an artificial state with an extremely reduced Young’s modulus of 1.000 MPa. When the elements are heated over 1450 °C the material state is changed to one with real material properties. Considering the melting, the command “TF” is used and a value of 1450 °C is chosen. This command causes a reset of the accumulated plastic strains when the chosen temperature (melting temperature) is achieved. In doing so, a reset of the hardening is caused, as well. Isotropic, kinematic and mixed hardening models are selected.

The thermo-mechanical calculation is uncoupled in two sequentially calculated steps. At first, the temperature distributions for all discretised time-steps are calculated. To model the high thermal gradients the backwards-difference method is used. Afterwards, the resulting mechanical behaviour is calculated with the load-step method. The dead-weight of the plate is not taken into account.

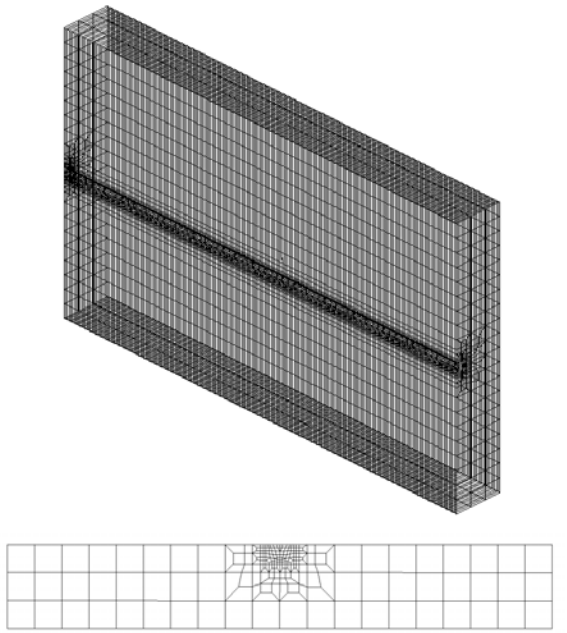

Fig. 2 The surface and a cross section of the mesh

The material properties of the material used can be found in [1]. The hardening was modelled for strains up to 20 %. For the filler material the same properties than for the base material are used. The used calculation methods which calculate the temperature distributions at the undeformed shape make it necessary to model the density only for the room-temperature, but the heat conductivity and the specific heat capacity temperature dependent.

The heat input is distributed using the Goldak heat source [8]. The temperature-fields are calibrated to the isothermal line of the melt pool which can be observed in a micrograph and to the measured temperatures of the thermo-couples.

The modelled thermal boundary conditions include heat losses on all surfaces by radiation (Stephan-Boltzmann law) and convective losses (25 W/m^2K). To model the mechanical constraints, the experimental plate is supported on three pins, three nodes are modelled rigid in depth direction and with soft springs in horizontal direction.

RESULTS OF THE NUMERICAL MODEL

TEMPERATURE FIELD

A necessary precondition to predict the mechanical behaviour of welded components is a reliable modelled temperature-field. Fig. 3 and fig. 4 show the measured and the modelled temperatures in two points in a distance of 3 mm and 6 mm next to the weld centre during welding the two layers. Although the first graph indicates that the first heat source is modelled a bit wider and the heat source for the second layer is modelled smaller than in the experiment, it is accurate enough to describe the mechanical behaviour. The variations may cause a small shift of the observed peaks, but are not sensitive to the principal mechanical behaviour.

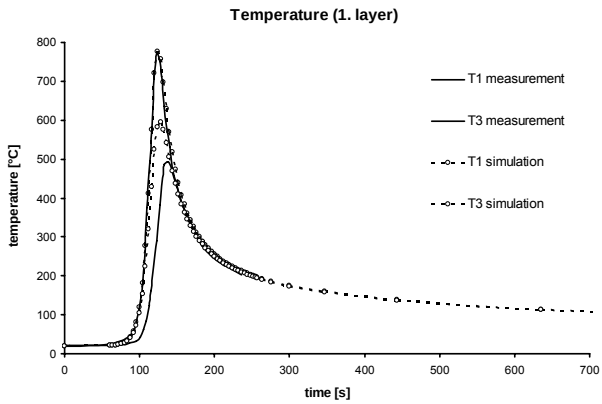

Fig. 3 Comparison of the simulated and measured temperatures during the 1st layer

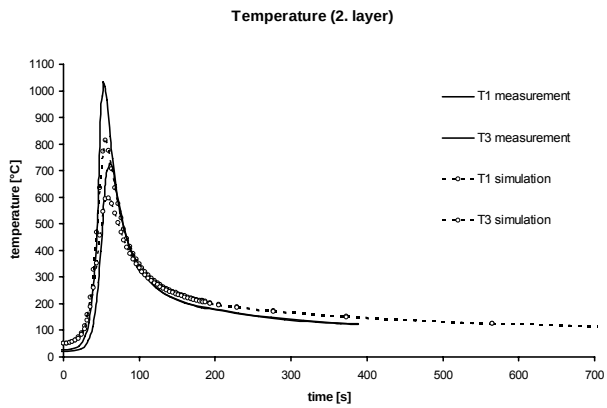

Fig. 4 Comparison of the simulated and measured temperatures during the 2nd layer

MECHANICAL BEHAVIOUR OF THE PLATE

A comparison of measured and calculated angular welding distortions can be found in [7]. A good agreement between the measured and modelled deformations is described. The used hardening model has only little influence on the calculated deformations. Nevertheless, the corresponding calculated stresses of all former models with different model assumptions vary widely.

Fig. 5 an Fig. 6 represent the calculated distributions of longitudinal and transverse residual stresses in a surface layer of the austenitic steel plate after welding of the second pass. The distribution of longitudinal residual stresses (Fig. 5) reveals clearly the lower magnitude (ca. 270 MPa) of the tensile residual stresses along the weld centre line in comparison with maximum magnitudes of 380 MPa on both sides of the weld seam.

Fig. 6 indicates that the distribution of transverse residual stresses is not symmetrical with respect to a middle line transverse to the weld seam. The maxima of tensile residual stresses are closer to one end of the seam. This result could be a consequence of the continuous welding process beginning at one end of the plate. In the middle of the seam a rather broad band of compressive residual stresses with a magnitude of ca. 50 MPa is noticeable, which is surrounded on both sides by tensile residual stresses with magnitudes up to 150 MPa.

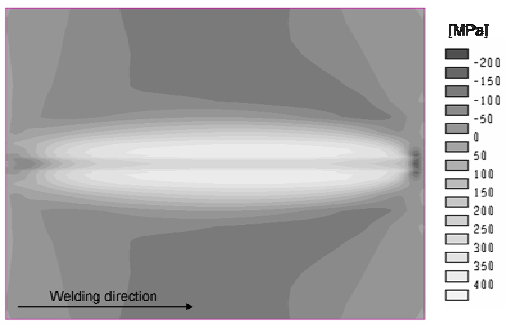

Fig. 5 Longitudinal residual stresses calculated with the materials law of isotropic hardening

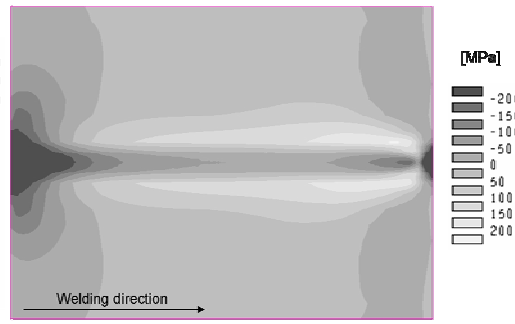

Fig. 6 Transverse residual stresses calculated with the materials law of isotropic hardening

Fig. 7 and Fig. 8 illustrate the distributions of longitudinal respectively transverse residual stresses over various cross sections. Especially the longitudinal stress component shows rather high magnitudes of tensile stresses just below the surface layer. Tensile stresses of the transverse component are found in somewhat deeper layers.

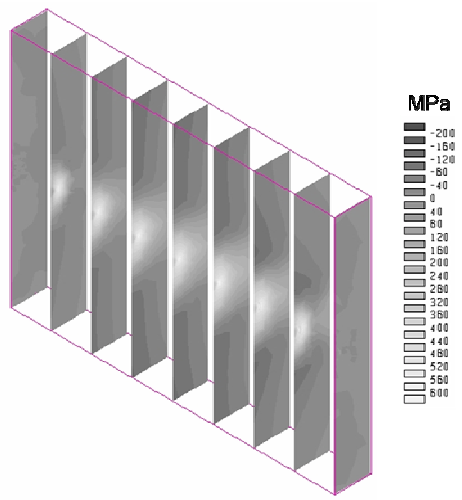

Fig. 7 Longitudinal residual stresses over various cross sections of the steel plate

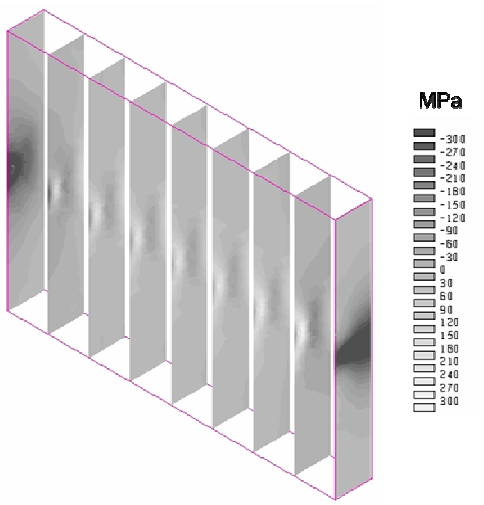

Fig. 8 Transverse residual stresses over various cross sections of the steel plate

Comparisons of calculations with different hardening models as well as with measured distributions are achieved with residual stress distributions along a line transverse to the weld seam in a distance of 90 mm from the end of the seam. Fig. 9 compares residual stress distributions measured by means of a hole drilling method in combination with electron speckle interferometry with a calculated distribution using the isotropic model assumption. This comparison between measured and calculated results is especially reasonable as the depth over which the stresses are integrated is with 1 mm exactly the same for the measurements and for calculations.

As can be seen three measurements reveal the typical maxima of tensile residual stresses with magnitudes between ca. 350 MPa and more than 400 MPa in distances of ca. 7 mm from the weld centre line. The measured tensile minima at the weld centre line are between nearly 200 MPa and nearly 300 MPa. Fig. 9 demonstrates a good agreement of the residual stresses calculated under the assumption of isotropic hardening with the measured ones. With one exception the measured peak stresses are a little bit lower than the calculated peak stresses of 380 MPa. The measured minimum tensile stresses at the weld centre line are also with one exception somewhat lower than the calculated stress at the weld centre line which remains at the value of the original yield strength of the material (ca. 275 MPa).

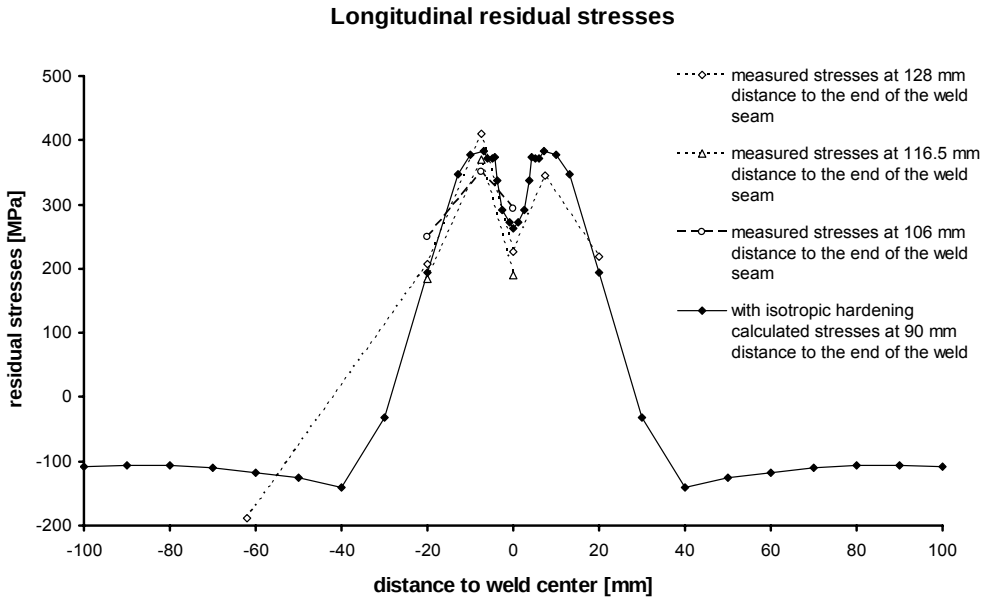

Fig. 9 Measured and calculated longitudinal residual stresses along a line transverse to the weld seam

The comparison of calculated and measured transverse residual stresses in Fig. 10 indicates a situation which is not as clear as for the longitudinal stresses. Only two of the measured residual stress distributions show stress minima in the compressive range at the weld centre line and are therefore in agreement with the calculated stresses. But the measurement in a distance of 128 mm from the end of the weld seam indicates a tensile stress maximum of more than 150 MPa at the weld centre line. This discrepancy to the other measured results could possibly be a consequence of the different distances of the measurements to the end of the seam because the distribution of the transverse residual stresses is asymmetric as already shown in Fig. 6. In addition it should be mentioned that other measurements by means of X-ray diffraction or neutron diffraction exhibited also tensile stress maxima of 300 MPa or at least 100 MPa in distances of ca. 10 mm from the weld centre line and a stress minimum in the compressive range at the weld centre line [2] and support therefore the calculated result in principle.

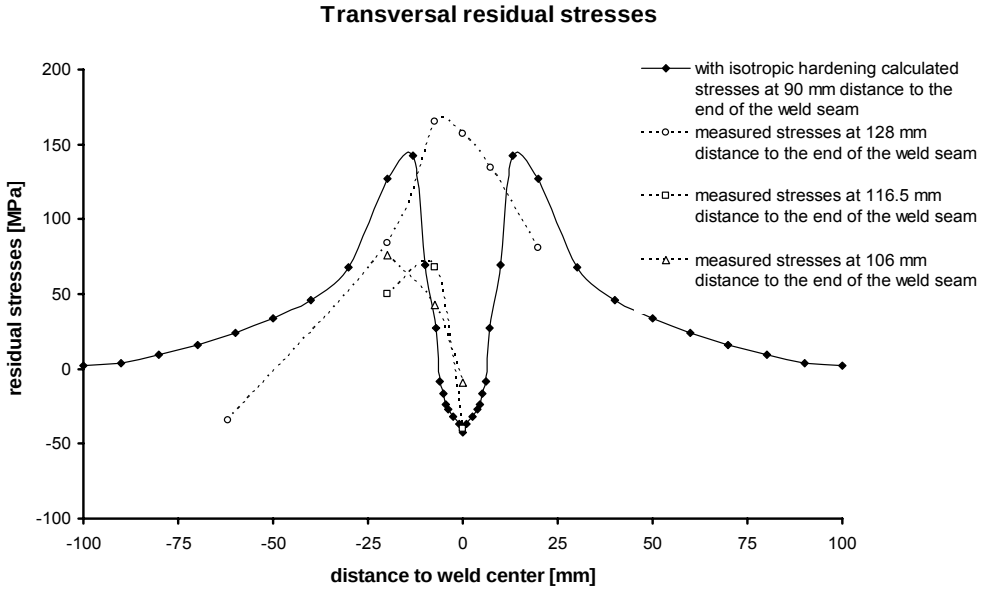

Fig.10 Measured and calculated transverse residual stresses along a line perpendicular to the seam

Residual stress distributions calculated with different hardening models are compared in Fig. 11 and Fig. 12. As illustrated in Fig. 11 calculations using the model of pure isotropic hardening result in the already cited tensile maxima of the longitudinal stresses of 380 MPa which are in good agreement with the measured maxima. The figure reveals clearly that all calculations with a combination of isotropic and kinematic hardening result still in tensile stress maxima in the HAZ. But these maxima become the lower the bigger the used percentage of the kinematic hardening model is. Calculations with the pure kinematic hardening model do not show tensile stress maxima in the HAZ, but a rather low horizontal plateau of tensile stresses (ca. 275 MPa) with somewhat higher values at the centre line, which overcome the flow stress of the material. Interesting enough calculations under the assumption of ideal elastic-plastic material behaviour exhibit almost the same residual stress distribution as calculations with kinematic hardening.

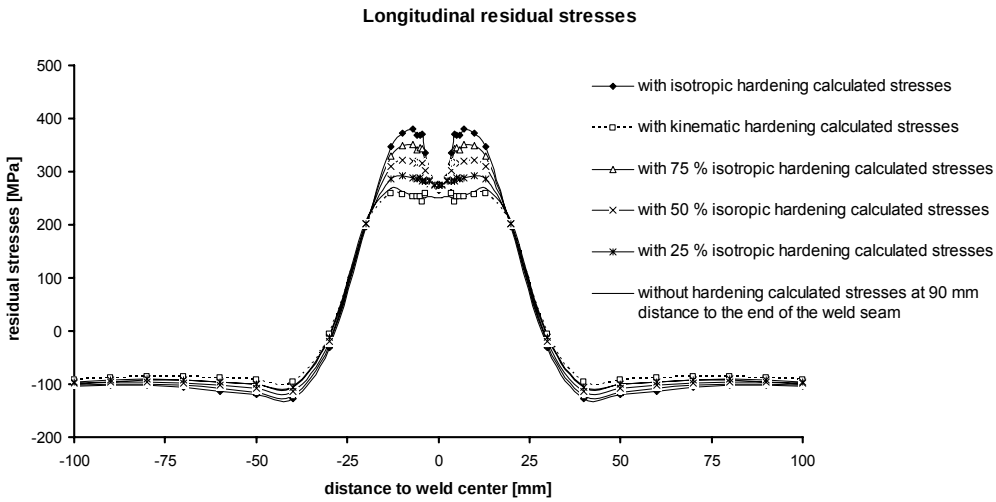

Fig. 11 Longitudinal residual stresses calculated with different material laws

As indicated in Fig. 12 the maximum tensile values of the transverse residual stresses are also lowered with an increasing percentage of kinematic hardening. The minimum of the transverse stresses at the weld centre line is still clearly in the compressive range if a percentage of 25 % kinematic hardening is taken in the calculation, but reaches only very small magnitudes in the compressive range with the pure kinematic hardening model.

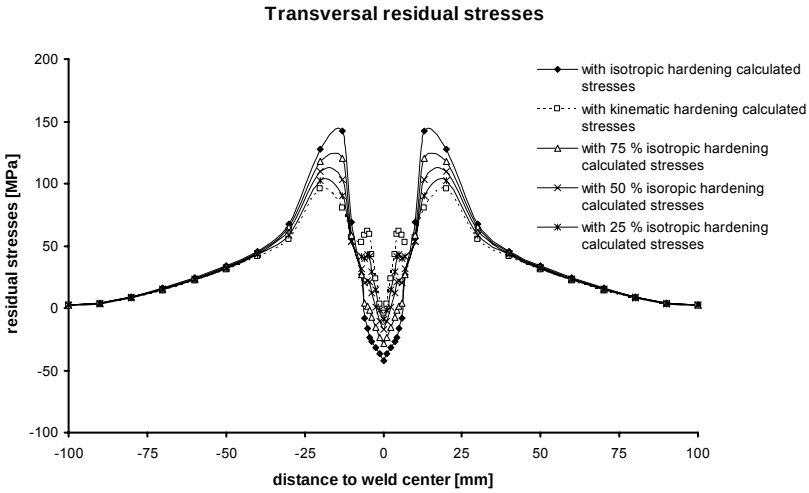

Fig. 12 Transverse residual stresses calculated with different material laws

Development of residual stresses and work hardening during welding, Mechanical behaviour during the process

The following diagrams illustrate the development of longitudinal and transverse stresses at various time intervals. All stress distributions are calculated along a line transverse to the seam in a distance of 90 mm from the end of the seam. They offer a good understanding of the interaction between stresses and work hardening in connection with the analogous diagrams of the isotropic hardening variables. It can be seen that the stresses in the weld seam and in the plastically deformed areas are limited at any time by the flow or yield stress. This flow stress depends upon temperature during heating and cooling and also on the work hardening occurring in the heating phase.

Fig 13 reveals the development of longitudinal stresses during welding of the first layer. A short time after the beginning of the welding process a rather broad band of compressive stresses (maximum magnitude 280 MPa) can be found on each side of the seam resulting after 247 s in the stress distribution shown in the figure, shortly before the maximum temperature is reached (271 s). After 299 s at the beginning of the cooling phase the compressive stresses are already reduced again and further on tensile stresses grow up in this area achieving a final magnitude of ca. 300 MPa (3000 s). This value is slightly higher than the original yield strength, indicating that work hardening has occurred (compare Fig. 17). The balancing compressive stresses in zones more remote from the seam increase at first during the cooling period and finally cover a wide range with somewhat lower magnitudes.

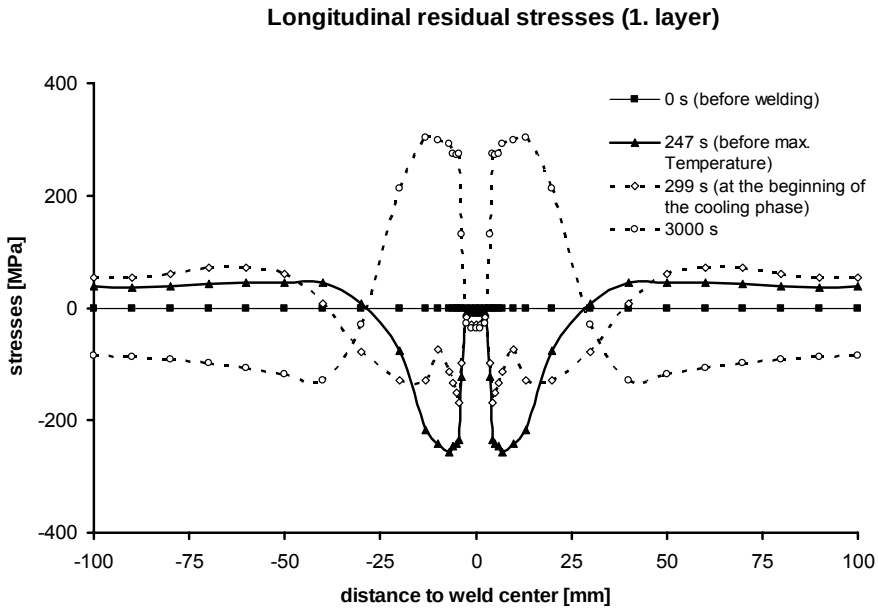

Fig. 13 Longitudinal stresses after selected time intervals during welding of the 1st pass

The progression of stresses during the second pass, indicated in Fig. 14, follows of course the same principles as after the first pass, but disagrees quantitatively. After the beginning of welding the residual stresses induced by the first pass are removed. As a consequence of the hindered thermal expansion compressive stresses develop during heating in a rather narrow zone on both sides of the weld seam. The compressive stresses attain their maximum magnitude of more than 300 MPa after 3245 s just before the maximum temperature is reached. With the beginning of the cooling period (3301 s) tensile stresses grow up in the seam and in the adjacent zones. It is interesting to see, that the magnitude of the tensile stresses in the weld seam remains at any time somewhat lower than the maximum magnitudes of the stresses in the HAZ. Towards the end of the cooling period these maximum magnitudes of the stresses in the HAZ grow more rapidly than the stresses in the weld seam and reach finally a value of 380 MPa, whereas the residual stress at the weld centre line stops at a value of 275 MPa, that is to say at the original yield strength. The balancing compressive stresses in areas more remote from the seam increase again at first during the cooling period and then cover a wider range with somewhat smaller magnitudes.

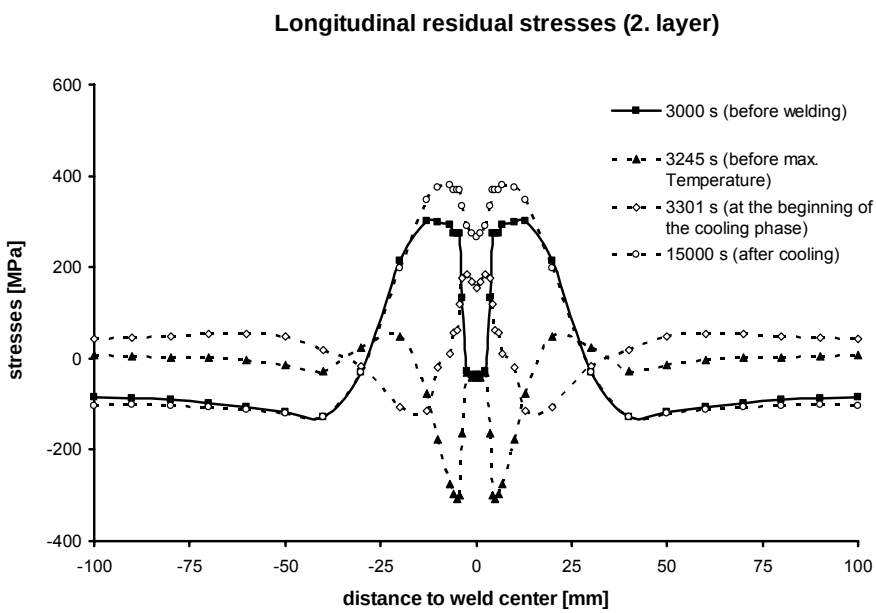

Fig.14 Longitudinal stresses after selected time intervals during welding of the 2nd pass

An evident feature of the stress distributions after the first and the second pass are the distinct compressive stresses in the HAZ shortly before the maximum temperature is reached (247 s in Fig 13 and 3245 s in Fig. 14). The development of these compressive stresses during the heating period is already important for the possibility to get finally residual stresses with especially high magnitudes in the HAZ. As the yield strength decreases with

increasing temperature the compressive stresses, which are increasing during heating, can reach this limit and produce plastic deformation and therefore work hardening in these zones. The produced work hardening will be still effective during cooling down and consequently tensile stresses respectively tensile residual stresses higher than the original yield strength can arise in the HAZ. In the weld seam no work hardening is produced and therefore tensile stresses grow up during cooling until they reach the limit of the original yield strength. The confirmation of the produced work hardening can be found in Fig. 17 and 18.

In Fig. 15 and Fig. 16 representing the transverse stresses at various time intervals the most evident effects are broad distributions of compressive stresses appearing at 247 s after the beginning of the first pass respectively after 3261 s. These compressive stresses develop already from the beginning of the weld passes as a consequence of the hindered expansion in the transverse direction. They cover the whole width of the plate. Their maximum magnitudes are for both passes lower than the analogous compressive longitudinal stresses. Therefore it is assumed that the transverse components of compressive stresses contribute less to plastic deformation and work hardening, the effects which have been already cited in connection with the longitudinal stresses. At the beginning of the cooling period the magnitudes of the compressive stresses become reduced. During the first pass tensile stresses start to grow then up to a maximum of ca. 150 MPa at 299 s on both sides of the weld seam, whereas the stresses in the seam itself remain in the compressive range. These maximum tensile stresses decrease again in further cooling to the final value of ca. 70 MPa (3000 s). After the reduction of these tensile maxima compressive stresses arise again in the second pass reaching a maximum magnitude of 270 MPa after 3261 s, just before the maximum temperature appears (3269 s). In the cooling period of the second pass tensile stresses begin to grow up in the HAZ as well as in the weld seam. In the HAZ the tensile stresses reach a maximum of ca. 270 MPa after 3301 s, whereas after a short period (20 s) of growing up to ca. 100 MPa the tensile stresses in the weld seam decrease very rapidly to low magnitudes of ca. 30 MPa after 3301 s. Until the end of the cooling phase (15000 s) the tensile stresses in the HAZ become also reduced to lower values (ca. 140 MPa) and the stresses in the weld seam come finally into the compressive range (ca. -40 MPa). These reactions could possibly be a consequence of angular distortion and of the temperature adjustment in areas more remote from the seam in the austenitic steel plate with its relatively low thermal conductivity.

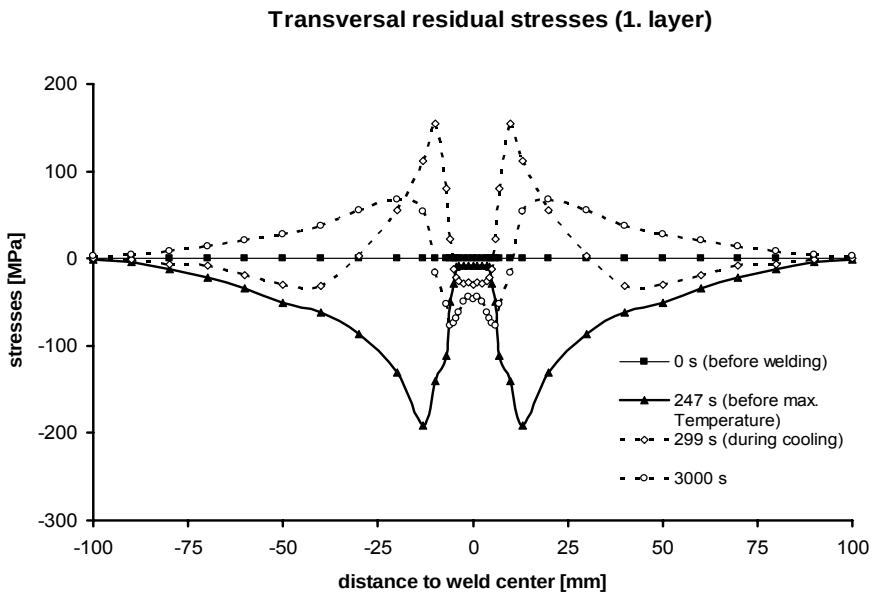

Fig. 15 Transverse stresses after selected time intervals during welding of the 1st pass

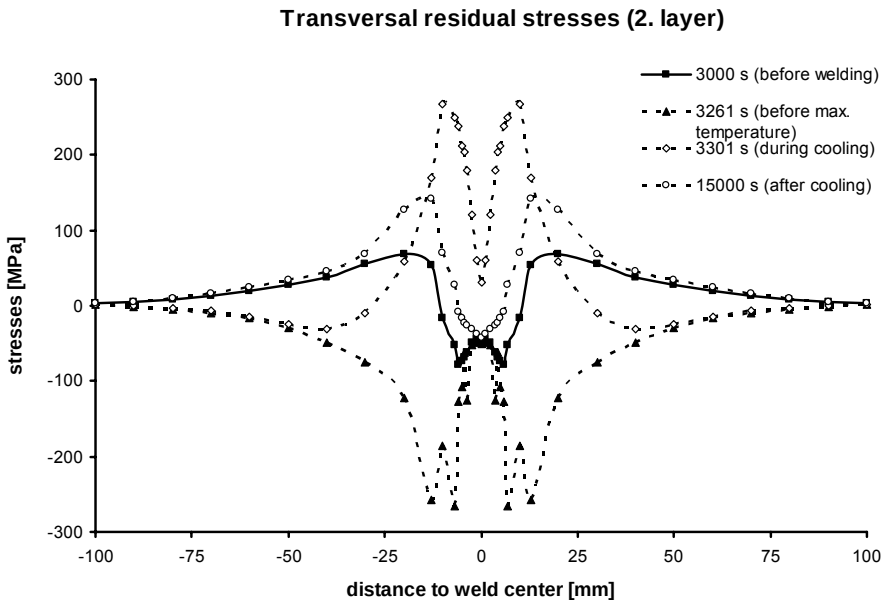

Fig. 16 Transverse stresses after selected time intervals during welding of the 2nd pass

Fig. 17 exhibits the temperature dependent and hardening dependent yield stress or flow stress at selected time intervals of the second pass. It confirms the already cited work hardening effects by increased flow stress values. During the first pass a relatively small increase of the yield stress is generated in the HAZ. The beginning of the second pass (3000 s) is denoted by this increased flow stress which is reduced again during the heating of the second pass and at the maximum temperature the flow stress in the weld seam becomes zero (3269 s). At the beginning of the cooling period (3301 s) the flow stress has risen again. In the HAZ a small work hardening effect can already be realised increasing to the rather high flow stress value of 430 MPa at the end of the cooling period (15000 s). This maximum value indicates that even higher tensile residual stresses would have been possible than calculated by means of the isotropic hardening law. The flow stress of the weld seam remains in the range of the original value.

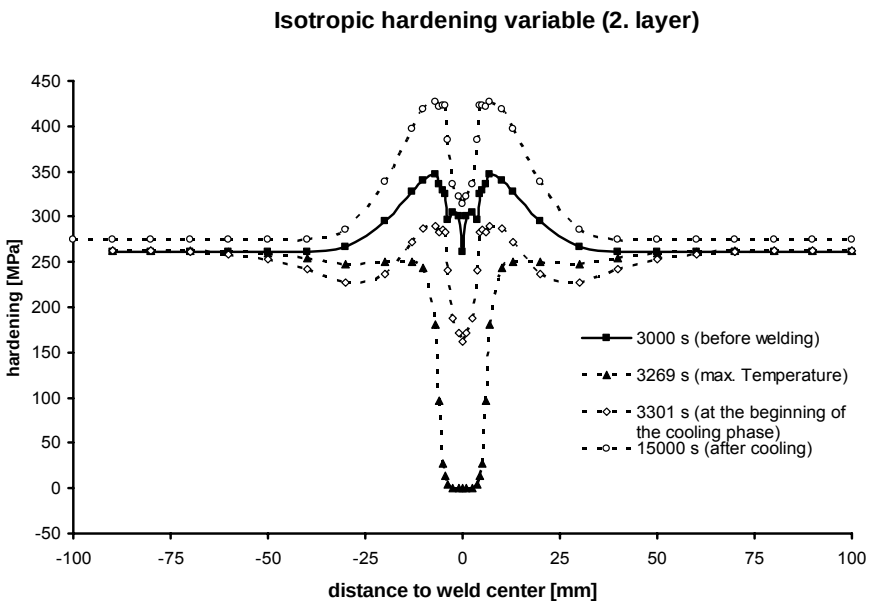

Fig. 17 Isotropic hardening variable after selected time intervals of the 2nd pass

The work hardening itself produced in the HAZ can be easily derived from Fig. 17 by subtracting at each temperature the temperature dependent flow stress from the value in Fig. 17. The work hardening fractions after different time steps of the second pass are indicated in Fig.18.

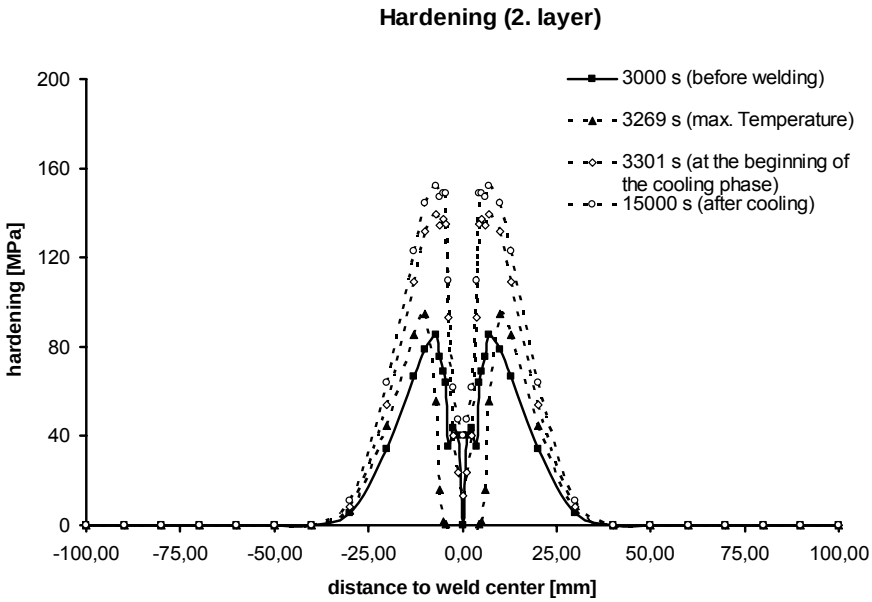

Fig. 18 Distribution of work hardening at selected time intervals

DISCUSSION

As a starting point for the discussion Fig. 19 exhibits the calculated von Mises stresses at several selected time intervals. The distribution of the stresses is very similar to the distribution of the longitudinal stresses, but has the advantage that an explanation of the different conflicting factors influencing the stresses during heating and cooling can be exposed more generally than for the individual stress components.

The individual factors are:

- development of compressive stresses in the HAZ due to thermal expansion during heating
- temperature dependent decrease of the locally present flow stress
- plastic flow and consequently work hardening in the HAZ
- development of tensile stresses due to shrinkage during cooling in the HAZ and after solidification in the weld seam

Fig. 19 indicates for instance that due to the reduction of the flow stress at the maximum temperature the von Mises stresses are appreciably lowered in the HAZ and are of course zero in the weld seam. During cooling, for instance after 3301 s, the von Mises stresses are enhanced again in the weld seam as well as in the HAZ as a consequence of shrinkage and

of the increasing flow stress with decreasing temperature. But in the HAZ the work hardening produced during heating is additionally effective and enables higher magnitudes of stresses than in the weld seam. Finally, after completed cooling the shrinkage stresses in the weld seam will be limited by the original flow stress, whereas the stresses near the fusion line in the HAZ can reach appreciably higher magnitudes due to the work hardening influence.

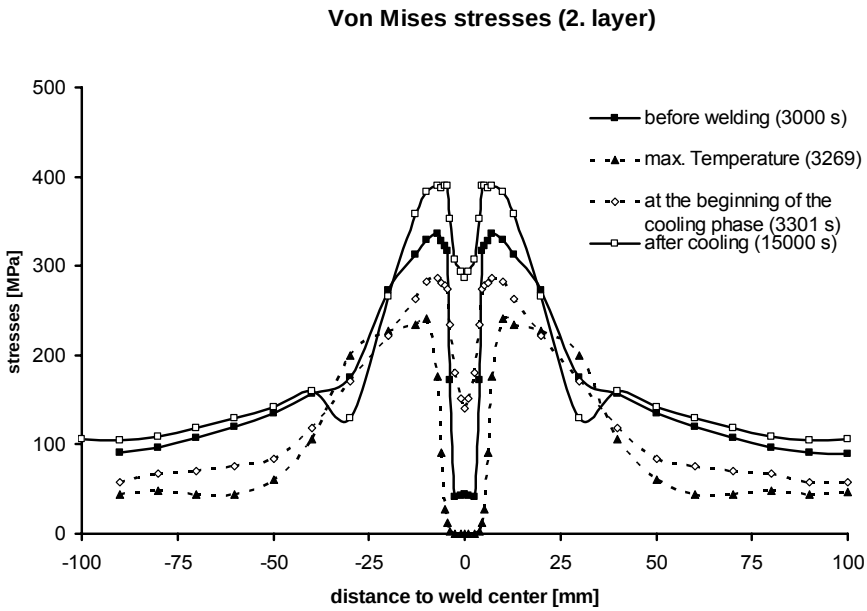

Fig. 19 Von Mises stresses after selected time intervals during welding of the 2nd pass

Concerning the cited hardening models for calculations the difference between both models is, that the kinematic hardening model takes into account the Bauschinger effect, whereas the isotropic model does not. That is to say, the kinematic hardening model considers the increase of compressive stresses during the heating period as a first load cycle and the opposite increase of tensile stresses during cooling as a second load cycle. Taking into account the Bauschinger effect is connected with the assumption that the beginning of plastic flow in the second load cycle (load reversal during cooling down) is lowered compared with the onset of plastic flow during the first load cycle (heating up). Fig. 20 offers a schematic model consideration and the quantitative rules for the Bauschinger effect. Consequently the kinematic hardening model does not take into account the increase of the flow stress due to work hardening in the first cycle and calculates a rather low flow stress or yield stress after completed cooling. The final tensile stresses will be limited by this relatively low yield strength. The results of all calculations using the kinematic hardening

law seam to indicate such a case: namely nearly constant tensile residual stresses with amounts in the range of the original yield strength at room temperature.

To take into account the influence of the Bauschinger effect is really necessary for cyclic plastic deformations at room or low temperatures, especially for materials with a high strain hardening exponent as for instance austenitic steels. But if the Bauschinger effect cannot be effective due to high working temperatures, as in welding, the error by using the kinematic hardening model will otherwise be especially substantial for materials with a high hardening coefficient.

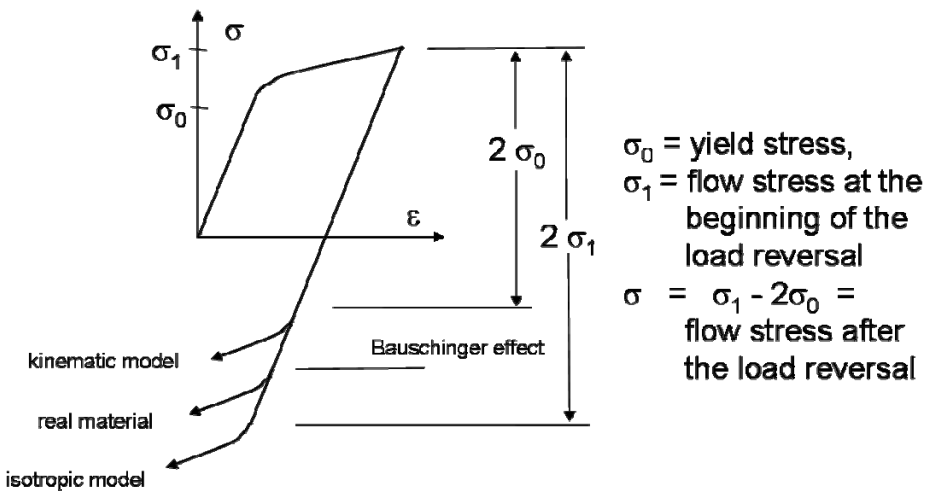

Fig. 20 Schematic model consideration of the Bauschinger effect [9]

Therefore, for calculations of residual stresses as a consequence of welding the isotropic hardening model should be used. It is able to account for even strong work hardening effects during the heating process and increased yield strength values can be anticipated during cooling down and finally at room temperature in the hardened HAZ close to the weld seam. Consequently the developing tensile stresses are limited only by these enhanced yield strength values and can become higher than with the kinematic hardening model. The measured and calculated maxima of the tensile residual stresses in the longitudinal direction can be understood in this way.

An additional proof for the suitability of calculations using the isotropic hardening model is the good agreement of the results in Fig. 21with the given materials data. According to Fig. 21 the maxima of the accumulated plastic strain are in the HAZ and represent ca. 5.7 %. A list of work hardening data for the austenitic steel given for the IIW Round Robin indicates a yield strength of 419 MPa at room temperature after a plastic deformation with a strain of 5 % [1]. Magnitudes of nearly 400 MPa of the maximum tensile stresses are obviously consistent with this yield strength value.

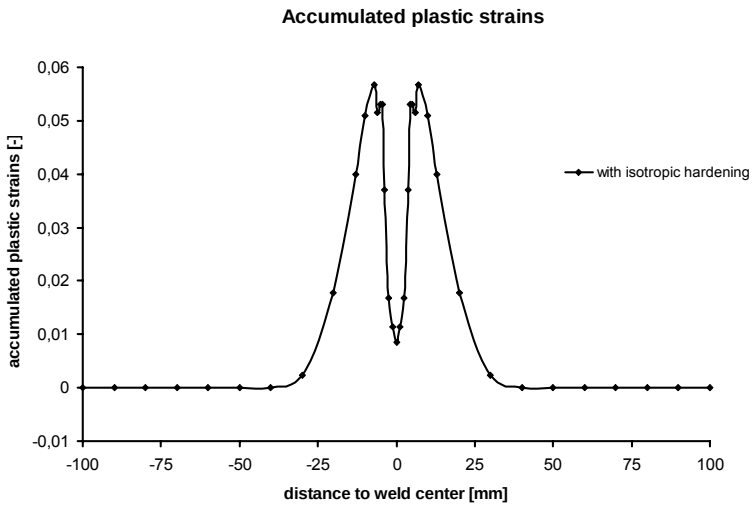

Fig. 21 Accumulated plastic strains

As mentioned, a comparison of measured distributions of transverse residual stresses with results calculated under the assumption of isotropic hardening indicates an agreement in principle. Distributions of transverse residual stresses computed by using the kinematic hardening model or the isotropic hardening model do not show fundamental qualitative discrepancies, however noticeable quantitative discrepancies. As additionally discrepancies exist between measured results, the comparison with the calculated transverse residual stresses cannot provide a supplementary substantial prove of the specific suitability of the isotropic hardening model.

CONCLUSIONS

Comparisons with verified measured residual stress distributions indicate:

- Calculations of residual stresses using the pure kinematic hardening model can neglect tensile stress maxima in a welded plate of an austenitic steel and offer instead of peak values a plateau of tensile stresses with appreciably lower magnitudes,
- but also calculations with a mixture of 25 %, 50 % or 75 % kinematic hardening and isotropic hardening underestimate the highest residual tensile stresses of the welded steel plate in this order more and more.
- The reason is, that it is obviously not correct to take into account the Bauschinger effect by assuming kinematic hardening behaviour, as this effect is not active in areas heated highly enough.
- Consequently the work hardening in the HAZ of the welded plate will not be considered as a process finally enhancing the yield strength at room temperature. The

tensile stresses increasing with the decreasing temperature will finally be limited by an incorrect low yield strength.

- As especially high tensile residual stresses may have rather detrimental influences in welded components, an underestimation by calculations must be regarded to be dangerous.
- Therefore calculations with the isotropic hardening model should be used for residual stress investigations in welded joints.
- It could be shown that such calculations can result in a very good agreement with measured residual stress distributions.
- The results of calculations of distortions due to welding are nearly independent of the model for the hardening behaviour of the material.

REFERENCES

[1] J.J. JANOSCH: „IIW Round Robin Protocol for Residual Stress and Distortion Prediction, Phase II (Proposal Rev. 1)“, *IIW-Document IIW-X/XV-RSDP-59-0.1.*

[2] H. WOHLFAHRT AND K. DILGER: “New results of the IIW Round Robin Residual Stress Measurements”. Report on the Experimental Round Robin Tests on Residual Stresses 2008. *IIW-Document IIW-XIII-2241-08, IIW-XV-1283-0.*

[3] J.J. JANOSCH: „Round Robin phase II – 3D modelling. Updated results“, *IIW Document II-X/XIII/XV-RSDP-114-05.*

[4] J.J. JANOSCH: “International Institute of Welding work on residual stress and its application to industry“, *International Journal of Pressure Vessel and Piping,* 85(2008) pp. 183-190.

[5] T. MANNINEN ET AL.: “Large-strain Bauschinger effect in austenitic stainless steel sheet”, *Materials Science and Engineering* A 499 (2009) pp. 333-336.

[6] M.C. MATAYA AND M.J. CARR: “The Bauschinger Effect in a Nitrogen-strengthened Austenitic Stainless Steel”, *Materials Science and Engineering* 57(1983) pp. 205-222.

[7] H. WOHLFAHRT: ”New calculations checking an adequate materials law. New results on distortion measurements”. Report on the Round Robin Tests on Residual Stresses 2009. IIW Document IIW-X-1668-09, IIW-XIII-2291-09, IIW-XV-1326-09.

[8] J. GOLDAK: “A new finite element model for welding heat sources”, *Metallurgical and Materials Transactions B,* 15(1984) pp. 299-305.

[9] L. SCHREIBER: Vorlesung “Plastizitätstheorie 2”, Universität Kassel, 2009.